Irreversibility and chaos: Role of long-range hydrodynamic interactions in sheared suspensions

Bloen Metzger[1] and Jason E. Butler[2]
[1]*IUSTI-CNRS UMR 6595, Polytech'Marseille, 13453 Marseille Cedex 13, France*
[2]*Department of Chemical Engineering, University of Florida, Gainesville, Florida 32611, USA*
(Received 6 July 2010; revised manuscript received 16 August 2010; published 30 November 2010)

Non-Brownian particles suspended in an oscillatory shear flow are studied numerically. In these systems it is often assumed that chaos (due to the long-range nature of the hydrodynamic interaction between particles) plus noise (contact or roughness) lead to irreversible behavior. However, we demonstrate that the long-range hydrodynamic interactions are not a source, nor even a magnifier, of irreversibility when coupled with non-hydrodynamic interactions. Additionally, analysis reveals that the apparent anisotropy of the particle diffusion is due to coupling of the shear flow and transverse diffusion.

DOI: 10.1103/PhysRevE.82.051406 PACS number(s): 83.80.Hj, 47.15.G−, 47.57.E−

I. INTRODUCTION

Particle dispersion in sheared suspensions has been a subject of intensive research since 1977 [1]. Even though many theories have been put forth to explain this phenomenon, some confusion remains about its physical origin. When the interactions are solely determined by Stokes flow, which is termed the "pure-hydrodynamic limit" (i.e., only hydrodynamic forces are present and the Reynolds number is zero), the motion of the particles is deterministic and expected to be reversible [2]. The observed dispersion was attributed to excluded volume effects [3]. In a shear flow, when two spheres approach, the minimum separation can be less than 10^{-4} of their radius. Surface asperities can therefore induce particle displacement, forcing particles from their reversible path; particles separate on streamlines further apart than on their approach. Within this frame, diffusivity coefficients were obtained using a path integration method [4]. Brady and Morris [5] extrapolated a scaling theory valid for dilute systems to describe shear-induced self-diffusion in the concentrated regime.

Drazer *et al.* [6] showed that the complex dynamics of sheared suspensions can be characterized as a chaotic motion in phase space. Chaos when coupled to any source of noise ensures that reversal of the velocities of all the particles does not, in practice, lead to a time-reversed motion; any small perturbation in the state of the system grows exponentially in time. Thus, small perturbations (weak Brownian motion, particle roughness, or any finite-ranged force), which are inevitably present in a real system [7], will grow. It is thus impossible for the system to retrace its dynamical path upon reversal.

For sedimenting particles, Jánosi *et al.* [8] demonstrated that chaos arises from long-range hydrodynamic interactions (LRHIs). The chaotic nature of hydrodynamic interactions was also invoked [9] to account for the observed irreversible behavior in sheared suspension. Sierou and Brady [10] mentioned that it is not clear whether the presence of an interparticle force is necessary for diffusive motion to appear. Marchioro and Acrivos [11] also suggested that in the absence of an interparticle force, diffusive like characteristics could be present owing to the chaotic nature of the many-body hydrodynamic interactions.

However, recent experimental studies [12] have shown that the extent of the irreversibility is strongly correlated with the particle roughness, as also found for the interaction between only two particles [3,13]; in the latter case, since only two particles are involved, one cannot invoke chaos to account for the irreversible motion of the particles. The microscopic origin of particle dispersion thus remains obscure. Several fundamental questions persist regarding the role of the long-range hydrodynamic interactions in generating chaos and whether contacts should be considered just a source of noise or as a primary source of irreversible displacements.

This paper reports on a simple numerical model developed to inquire specifically about the role of the long-range hydrodynamic interactions on particle dispersion and chaos in sheared suspension. In contrast to the case of sedimentation, we find that the long-range hydrodynamic interactions tend to damp the particle dispersion and do not contribute to the chaoticity of the system.

II. NUMERICAL MODEL

A minimal model is used to describe suspensions of non-Brownian particles within a periodic shear flow. A total of N particles is initially distributed in a monolayer with nonoverlapping positions to give the desired areal fraction; simulating a monolayer of particles provides substantial savings in computational time while maintaining an accurate description of the relevant physics. The particle positions are periodic in the flow (x) direction and are constrained in the z direction by solid walls. The velocity of particle n, $\mathbf{u}_n$, is the sum of the advection velocity due to the shear flow, the velocity disturbances generated by the straining flow, and the motion created by interparticle forces,

$$\mathbf{u}_n = \dot{\gamma} z_n \sin(\omega t)\mathbf{e}_x + \sum_{m\neq n}^{N} \bar{\mathbf{U}}_m(\mathbf{x}) + \frac{1}{\xi}\sum_{m\neq n}^{N} \mathbf{F}_{nm}, \qquad (1)$$

where $\bar{\mathbf{U}}_m$ is the disturbance velocity due to a sphere located at $\mathbf{x}_m$ at a distance $\mathbf{x}=\mathbf{x}_m-\mathbf{x}_n$ from the sphere n. The leading-order description is used to account for the LRHIs between particles [14],

$$\bar{\mathbf{U}}_i(\mathbf{x}) = \left[\mathbf{xx}\left(-\frac{5a^3}{2x^5} + \frac{5a^5}{2x^7} \right) - \mathbf{I}\frac{a^5}{x^5} \right] \cdot \mathbf{E} \cdot \mathbf{x}, \tag{2}$$

where $\mathbf{E}$ is the rate of strain and a is the particle radius. To account for steric effects, a pairwise-repulsive force (RF) is included. The repulsive force exerted by particle m on particle n is

$$\mathbf{F}_{nm} = \begin{cases} -F_0 \dfrac{\mathbf{x}}{|\mathbf{x}|} & \text{if } |\mathbf{x}| \le 2a \\ 0 & \text{if } |\mathbf{x}| > 2a, \end{cases} \tag{3}$$

where F_0 denotes the amplitude of the repulsive force and ξ in Eq. (1) is the Stokes resistance. We set $F_0/\xi = 1$. Other values were tested for F_0 as well as other repulsive potentials [15], but all returned similar results.

This numerical model represents a rudimentary description relative to the substantially more accurate three-dimensional models existing in the literature [4,10]. However, this version includes long-range hydrodynamic interactions and captures the many-body hydrodynamic interactions at the level of multiple summed pairs. The model does not include lubrication forces purposely as we aim to investigate whether long-range hydrodynamic interactions engender chaos; as a result, effects such as closed trajectories of a pair of particles in close proximity are not observed from simulations at the level of Eqs. (1)–(3). However, comparisons of this model with a code containing multiple reflections and the velocity disturbance created by the repulsive force (i.e., Stokesian dynamics without lubrication interactions) demonstrated qualitative agreement in all respects, so the present model is used for the sake of simplicity.

Equations (1)–(3) are solved numerically. Knowing the positions of the particles at time $t=0$, the subsequent positions of each particle are calculated using a variable order Adams-Bashforth-Moulton solver. Simulations were performed with up to $N=50$ particles that were tracked over 25 cycles at strain amplitudes γ_0 between 0.25 and 3. One strain unit corresponds to a relative displacement of the cell walls equal to their separation distance. The total accumulated strain after n cycles is $\gamma = 4n\gamma_0$, as γ_0 is the strain for a quarter cycle.

III. RESULTS

We first present results from simulations of 50 particles that neglect the LRHIs. We thus consider a suspension of hard spheres driven by an external shear flow where interaction between particles only occurs through the repulsive potential given by Eq. (3). At very short times, the mean-square particle displacements, $\langle xx \rangle$ and $\langle zz \rangle$, increase rapidly and then transition to a linear regime for $\gamma \ge 20$ as seen in Fig. 1(a). The transient regime, as previously observed [10,16], corresponds to the rearrangement of the initially random configuration into a self-organized one. The slopes of the mean-square particle displacements for $t > 20$ define the dimensionless diffusivities $D_x^* = \langle xx \rangle / 2a^2\gamma$ and $D_z^* = \langle zz \rangle / 2a^2\gamma$ plotted in Fig. 1(b). The diffusion coefficients along, D_x^*, and perpendicular, D_z^*, to the flow direction rapidly increase with strain amplitude.

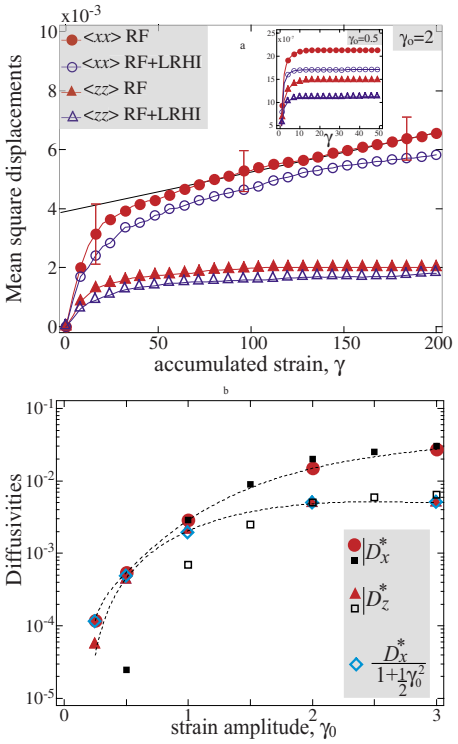

FIG. 1. (Color online) (a) Mean square displacements along and perpendicular to the flow direction, $\langle xx \rangle$ and $\langle zz \rangle$, versus accumulated strain, γ, for $\gamma_0 = 2$ and in the inset for $\gamma_0 = 0.5$. (b) Diffusivity coefficients, D_x^* and D_z^*, and normalized diffusivity coefficient $D_x^*/a^2(1+\frac{1}{2}\gamma_0^2)$ (which accounts for the advection-diffusion coupling) versus strain amplitude, γ_0. Squares are from experiments [9].

These numerical results closely agree with the experimental data of Pine *et al.* [9] and successfully predict the transition of the particle dispersion at $\gamma_0 \approx 1$. For strain amplitudes smaller than 1, the system self-organizes into a nonfluctuating quiescent state [see inset of Fig. 1(a)] as suggested by the experiments of Corté *et al.* [16]. The structure of the self-organized state varies according to the concentration and the strain amplitude as demonstrated by Stokesian dynamics simulations [15].

An advection-diffusion coupling occurs when diffusion takes place in a shearing flow. In a channel, the sheared velocity profile interacts with cross channel diffusion to augment the dispersion along the channel. This effect, first studied by Taylor [17], was solved analytically in the specific case of a periodic shear flow and for a Brownian diffusion process [18]. The resulting effective diffusivity which arises from this coupling is $D(1+0.5\gamma_0^2)$, where D is the bulk isotropic diffusion coefficient. Normalizing D_x^* by $(1+0.5\gamma_0^2)$ collapses the points onto those of D_z^* as shown in Fig. 1(b). Hence, the larger diffusion coefficient measured along the flow direction does not arise from an intrinsic anisotropy of the particle diffusivity but more simply results from advection-diffusion coupling.

To test the effect of LRHIs, Eqs. (1)–(3) are solved fully including all terms. A striking result is that the mean-square

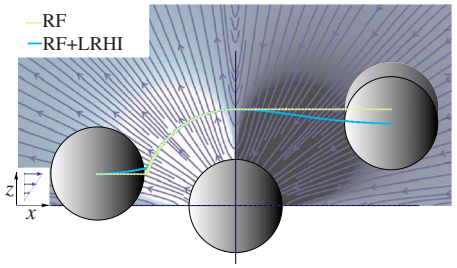

FIG. 2. (Color online) Effect of the LRHI on the relative trajectory of a pair of particles embedded in a simple shear flow. When in recession, the tensile normal stress brings the particles closer. The streamlines and the color scale represent, respectively, the flow disturbance [Eq. (2)] and the pressure field generated by the particle located at the origin.

displacements [see Fig. 1(a)] remain unchanged when the LRHIs are included. In fact, the simulations involving both repulsive forces and long-range hydrodynamic interactions generate slightly smaller particle mean-square displacements. This slight damping of the particle dispersion process may be understood considering the fore-aft symmetry of the hydrodynamic interaction between particle pairs, specifically the tensile normal stress of pairs when in recession [4,5]. Figure 2 illustrates this phenomenon. When particles are in recession, the LRHI is attractive. Not including the LRHI suppresses this effect and the resulting overall particle dispersion is larger.

However, this two-particle scenario omits the role of multiple particles colliding while also interacting hydrodynamically, which has been cited in the literature as a source of chaoticity [6,9,10,20]. To explore the role of LRHI on the chaoticity of multiple particles, simulations are undertaken with six particles; formally, the N-body problem only requires more than two particles to exhibit chaotic trends. Five hundred initial configurations are used and only those simulations that resulted in no particle contacts are retained within the analysis. Following Refs. [6,8,19], each initial condition is simulated twice, with two slightly different initial configurations, A and B. Configuration B is prepared from configuration A by displacing each particle in a random direction by a small distance ϵ. The Euclidian distance between these two simulations is computed in phase space as $l=\sqrt{\frac{1}{N}\Sigma_{i=1}^{N}(x_i^A-x_i^B)^2+(z_i^A-z_i^B)^2}$. In chaotic systems, l grows exponentially as $\epsilon e^{\lambda\gamma}$, where λ is the largest Lyapunov exponent. For three particles settling in a viscous fluid, Jànosi *et al.* found $\lambda\approx 0.04$, where γ corresponds to time, not strain, in their results. The positive value of the Lyapunov exponent clearly indicates chaos. Conversely when the particles solely interact through LRHI in periodic shear, the separation distance between two initially perturbed simulations remains unchanged as shown in Fig. 3(a). The corresponding Lyapunov exponent is too small ($\lambda<10^{-7}$) to observe chaotic behavior in the time frame of the simulations. This result is independent of the magnitude of the initial perturbation.

The separation distance is also evaluated for simulations of $N=50$ particles. This time, contact between the particles is allowed and simulations with and without LRHIs are compared. Figure 3(b) shows the exponential increase of the

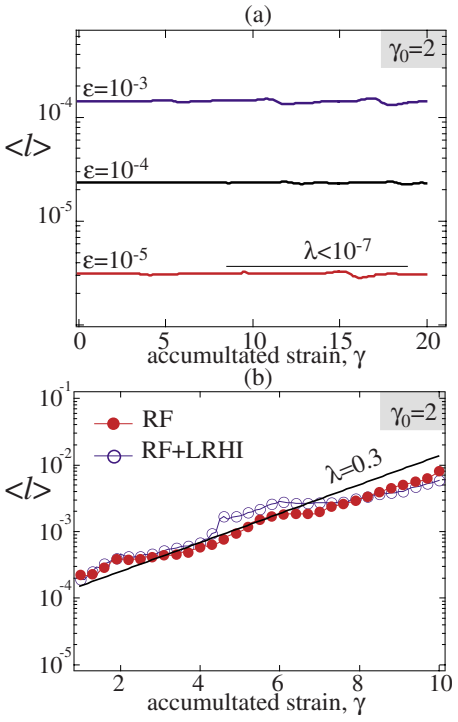

FIG. 3. (Color online) Separation distance, l, versus accumulated strain, γ, for a strain amplitude of $\gamma_0=2$. (a) Simulations are performed with $N=6$ particles interacting solely through LRHI. Different magnitudes of the initial perturbation, ϵ, are tested. (b) Simulations are performed with $N=50$ particles. Both sets of simulations (RF or RF+LRHI) started with the same initial positions.

separation distance, l, with accumulated strain amplitude, γ. The positive growth rate, $\lambda\approx 0.3$, indicates a chaotic behavior. Note that the slope or chaoticity remains the same when neglecting the LRHIs.

IV. CONCLUSION

We have examined the nature of particle dispersion in sheared suspension of non-Brownian particles submitted to a periodic flow using a simple numerical model including a repulsive potential (to avoid particle overlap) and long-range hydrodynamic interactions (to capture the many-body and long-range nature of the hydrodynamic interactions between particles). In the studied range of parameters, three major conclusions can be made:

(i) Long-range hydrodynamic interactions are not a source of irreversibility nor even a magnifier of irreversibility when coupled with nonhydrodynamic interactions. In fact, as a result of the tensile normal stress between pairs when in recession, LRHIs damp the particle dispersion.

(ii) Long-range hydrodynamic interactions do not generate chaos in sheared suspension. If the particles solely interact through LRHI, the particle motion is reversible since the Stokes equations are linear and, as we have shown, insensitive to perturbations.

(iii) A minimal model, involving the particle steric effect only, can successfully predict the experimentally observed transition of the particle dispersion at $\gamma_0\approx 1$.

These results provide a perspective on sheared suspensions that differs fundamentally from that of sedimenting suspensions. In the latter case, the fluid flow is generated by the fall of the particles themselves and the ratio of the fluid flow disturbances (Stokeslets $\approx F/r$, where F is the body force acting on the particles) to the average velocity of the particles (mean settling velocity $\approx F/a$) is $\mathcal{O}(1)$ at one-particle diameter, $r=2a$, from any particle of the suspension. In sedimenting suspensions, these hydrodynamic interactions, which decay inversely with separation distance between the particles, indeed prevail [8,19,21]. Consequently, sedimenting particles (which solely interact through these long-range multibody hydrodynamic interactions) constitute a chaotic system. This was clearly demonstrated by Jánosi *et al.* [8].

Sheared suspensions are fundamentally different. This time, an external flow is imposed and the ratio of the disturbances (stresslets $\propto a^3E/r^2$), to the mean particle velocity ($\propto \dot{\gamma}L$), where L is the cell wall distance, is $\mathcal{O}(a/L)$ for $r=2a$. These weaker interactions, which decay as the square of the inverse separation distance, do not generate chaos.

The main constraint driving the system may thus more likely be stated as *particles cannot overlap*. This would explain why exceedingly simple descriptions such as the recent collision-induced model [16,22], which does not include any hydrodynamics, or the one presented here largely capture the dynamics observed in experiments. This also corroborates recent observations that the extent of the irreversibility strongly correlates with particle roughness [12,13]. To avoid particle overlap, one can use, as we did, a repulsive potential. Dispersion of the particles then naturally occurs as this interaction is by essence irreversible. Another candidate to prevent particles from overlapping is lubrication. Lubrication is a reversible interaction on account of the Stokes equations; it may nonetheless be a source of chaos. We plan to address this question in future work.

ACKNOWLEDGMENTS

We thank D. Bartolo for having thoughtful discussions. Visits were supported by the Partner University Fund on particulate flows, Aix-Marseille Universite (U1), and ANR JCJC SIMI 9.

[1] E. C. Eckstein, D. G. Bailey, and A. H. Shapiro, J. Fluid Mech. **79**, 191 (1977).
[2] I. E. Zarraga and D. T. Leighton, Phys. Fluids **13**, 565 (2001).
[3] P. A. Arp and S. G. Mason, J. Colloid Interface Sci. **61**, 44 (1977).
[4] F. R. Da Cunha and E. J. Hinch, J. Fluid Mech. **309**, 211 (1996).
[5] J. F. Brady and J. F. Morris, J. Fluid Mech. **348**, 103 (1997).
[6] G. Drazer, J. Koplik, B. Khusid, and A. Acrivos, J. Fluid Mech. **460**, 307 (2002).
[7] J. F. Morris, Rheol. Acta **48**, 909 (2009).
[8] I. M. Jánosi, T. Tél, D. E. Wolf, and J. A. C. Gallas, Phys. Rev. E **56**, 2858 (1997).
[9] D. J. Pine, J. P. Gollub, J. F. Brady, and A. M. Leshansky, Nature (London) **438**, 997 (2005).
[10] A. Sierou and J. F. Brady, J. Fluid Mech. **506**, 285 (2004).
[11] M. Marchioro and A. Acrivos, J. Fluid Mech. **443**, 101 (2001).
[12] M. S. Ingber, A. A. Mammoli, and P. Vorobieff, J. Rheol. **50**, 99 (2006).
[13] M. Popova, P. Vorobieff, M. S. Ingber, and A. L. Graham, Phys. Rev. E **75**, 066309 (2007).
[14] G. K. Batchelor and J. T. Green, J. Fluid Mech. **56**, 375 (1972).
[15] J. M. Bricker and J. E. Butler, J. Rheol. **51**, 735 (2007).
[16] L. Corté, P. M. Chaikin, J. P. Gollub, and D. J. Pine, Nat. Phys. **4**, 420 (2008).
[17] G. Taylor, Proc. R. Soc. London, Ser. A **219**, 186 (1953).
[18] W. R. Young, P. B. Rhines, and C. J. R. Garret, J. Phys. Oceanogr. **12**, 515 (1982).
[19] B. Metzger, M. Nicolas, and É. Guazzelli, J. Fluid Mech. **580**, 283 (2007).
[20] A. Deboeuf, G. Gauthier, J. Martin, Y. Yurkovetsky, and J. F. Morris, Phys. Rev. Lett. **102**, 108301 (2009).
[21] J. Park, B. Metzger, É. Guazzelli, and J. E. Butler, J. Fluid Mech. **648**, 351 (2010).
[22] L. Corté, S. J. Gerbode, W. Man, and D. J. Pine, Phys. Rev. Lett. **103**, 248301 (2009).